Study of wheat (*Triticum aestivum* L.) seed rehydration observed by the Dent generalized model and ^{1}H-NMR relaxometry

Magdalena Bacior[1]* and Hubert Harańczyk*[1,2]

[1]Department of Soil Science and Agrophysics, University of Agriculture in Kraków, Mickiewicza 21, 31-120 Kraków, Poland
[2]Institute of Physics, Jagiellonian University, Prof. S. Łojasiewicza 11, 30-348 Kraków, Poland

Abstract. The early stages of winter wheat (*Triticum aestivum* L.) seed hydration were monitored in order to improve our understanding of the molecular mechanisms of drought resistance. Investigations were carried out using gaseous phase hydration kinetics, sorption isotherm, and ^{1}H-NMR relaxometry. Hydration kinetics have shown that the mass increase could be fitted with a single exponential function. Two fractions of bound water were distinguished: very tightly bound water, $\Delta m/m_0 = 0.082 \pm 0.016$, and the tightly bound water fraction, $\Delta m/m_0 = 0.048 \pm 0.033$, with a hydration time $t^h_1 = (62 \pm 23)\ h$. The standard Dent's model which was used to fit the experimental data, was successfully applied but only for values of relative humidity smaller than $h < 0.9$. The sorption isotherm was better fitted using the generalized Dent's model, with the value of the b parameter equal to 0.947, the mass of the water saturating primary water binding sites equal to $\Delta M/m_0 = 0.0209$, and the fraction of unoccupied binding sites at $h = 1$ equal to $1/b_1 = 0.104\%$. Proton free induction decays registered for dry samples up to hydration level $\Delta m/m_0 = 0.128$ were better described by the Abragam function, whereas for a higher hydration level the Gaussian function sufficiently described the proton signal of the samples.

Keywords: drought resistance, wheat seed, hydration kinetics, sorption isotherm, Dent generalized model, Nuclear Magnetic Relaxation

1. INTRODUCTION

Wheat (*Triticum aestivum* L.) is one of the most important food crops in the world due to its high carbohydrate, protein, and fibre content. In addition to being a source of calories, wheat contains significant amounts of vitamins, minerals and antioxidants, such as carotenoids, phenolics, and phytosterols (Abdel-Aal and Rabalski, 2008; Shewry and Hey, 2015). This crop is of global food importance, second only to maize. Wheat is commonly used to produce flour, malt, and various food products, such as bread, pasta, and breakfast cereals (Yang *et al.*, 2021). In most societies, wheat provides 20-30% of the daily caloric intake as a major source of protein and starch (Lemmens *et al.*, 2019). In countries with temperate climates, wheat is the dominant cereal, with global production of about 690 million tonnes in 2010 – 2014 (Shewry, 2018) and 750 million tonnes in 2018 – 2021 (Mitura *et al.*, 2023).

Wheat seeds are desiccation-tolerant biological systems that can survive drastic dehydration, this is associated with the removal of cellular water over a long periods of time. Moisture has a significant effect on the quality of wheat grains (Ferreira *et al.*, 2012), as water activity determines the chemical, physical, and microbiological properties of the grain (Rockland and Beuchat, 1987). Seed survival is also affected by the storage temperature (Walters *et al.*, 2010; Ellis, 2022). A comprehensive knowledge of the correct seed moisture content is important as it increases seed longevity and reduces exposure to fungi during storage (Bradford *et al.*, 2018; Bewley *et al.*, 2013). Seed viability is halved for every 5°C increase in seed storage temperature (ranging from 0 to 50°C) and for a 1% decrease in seed moisture content, the storage life of a seed is doubled, for

© 2024 Institute of Agrophysics, Polish Academy of Sciences

*Corresponding author e-mail: magdalena.bacior@urk.edu.pl

seed moisture contents between 5 and 14% (Harrington, 1960; 1972). As the temperature and moisture content decreases, significant physical changes occur in the stored seed, depending on the combined effects of moisture and temperature (Walters, 1998).

Seed longevity ranges from decades to millennia (Walters *et al.*, 2005), with wheat seeds having a half-life of 5 to 10 years under ambient conditions and 40 to 60 years under more favourable conditions (Solberg *et al.*, 2020). Compared to recalcitrant seeds with a higher water content, wheat seeds are more drought tolerant and can be stored dry for long periods (Pammenter and Berjak, 2007). As orthodox seeds, wheat can maintain their viability at low water contents (between 2 and 5%) and can be distinguished from recalcitrant seeds by their smaller size (Yulianti *et al.*, 2020). They can be desiccated to a water content of between 0.03 and 0.08 g H_2O g^{-1} total mass (Walters and Maschinski, 2019).

Ellis *et al.* (1990, 2022) suggested that seed longevity is improved with progressive dehydration, and recommended that the storage of seeds at low water contents should be achieved with a relative humidity of 10-12% during drying at 20°C, irrespective of the storage temperature. By contrast, Vertucci *et al.* (1990, 1993, 1994) argued that the excessive drying of seeds could be detrimental, and that the optimum seed moisture content for preservation is influenced by temperature and decreases with increasing temperature. Thus, the recommended RH for the preservation of seeds at room temperature is approximately 20-25% RH.

Wheat seeds can withstand severe drought conditions by activating specific mechanisms during the dehydration process. They accumulate sugars, polyols, and amino acids (*e.g.*, proline), but also late embryogenesis abundant (LEA) proteins. These, together with non-reducing sugars, form an intracellular glass during seed dehydration (Chen, 2019). As the cytoplasm transforms into a glassy state, both the cytoplasmic uptake of molecules and the rate of the chemical reactions are reduced (Buitink and Leprince, 2008; Parihar *et al.*, 2016) due to the high level of viscosity which inhibits molecular diffusion (Burke, 1986). It is possible that the cytoplasm of dried seeds in a glassy state resembles a disordered solid with the physical properties of a liquid state (Buitink and Leprince, 2008). On the other hand, the glassy phase in biological systems preserves the structural integrity of the macromolecules, reduces deleterious reactions and increases the stability of enzymes (Slade and Levine, 1994), which has implications for seed longevity. The desiccation of orthodox seeds causes little cell shrinkage because the dry mass accumulated during maturation occupies the entire cell volume. By contrast, the desiccation of recalcitrant seeds results in significant cell shrinkage due to less pronounced space-filling reserves (Leprince *et al.*, 2017; Nadarajan *et al.*, 2023).

Some grain is stored after harvest, this reduces its quality. In general, wheat, like other cereals, is harvested dry, which extends its shelf life during storage. Therefore, a certain knowledge of hydration kinetics and sorption isotherms is essential for the proper design of drying and storage processes. Seed ageing rates are closely related to storage conditions, these determine the formation of a glassy phase (Walters, 1998). There is also the problem of accurately predicting the rates of moisture adsorption by wheat during storage (Casada, 2002). A certain knowledge concerning sorption isotherms provides vital information about the stability of the products, and their moisture content, which changes during storage (Samapundo *et al.*, 2007). Sorption isotherms are essential for predicting suitable storage conditions and also for modelling drying processes. These are difficult to determine because of the time consuming measurements required to establish the equilibrium conditions between the sample and the water vapour. At higher moisture values (water activity), there is a problem with the accuracy of the results, especially at higher values of the sorption isotherm, due to sample degradation (Blahovec and Yanniotis, 2008).

The aim of the measurements was to analyse the change in the molecular dynamics of the bound water in wheat grains as a function of hydration and also to determine an appropriate model to describe the sorption process in this biological sample. Many mathematical models have been proposed to describe sorption isotherms, such as the Brunauer-Emmett-Teller (BET) model (Brunauer *et al.*, 1938), the Guggenheim-Anderson-de Boer (GAB) model or the Dent model (Dent, 1977). The Dent model has been used successfully to describe biological systems such as Antarctic lichens, algae (Harańczyk *et al.*, 2008; Bacior *et al.*, 2017), DNA or DPPC liophilizates (Harańczyk *et al.*, 2010; 2016), as well as soil samples (Arthur *et al.,* 2015), but there is a problem with the correct fitting of data for more composed systems, such as seeds, where the Dent model correctly describes the sorption data but not in the whole range of the water activity (from 0 to 1). Therefore, the generalized Dent model has been proposed to describe the sorption isotherm in wheat seeds. Another method used to study the processes taking place in drastically dehydrated seeds is Nuclear Magnetic Relaxation (NMR), a non-invasive technique that provides precise values for the relaxation times of the protons that constitute the biological material and distinguishes the water fractions present in a sample. NMR is a valuable tool for detecting changes in the free induction decay (*FID*) signal in seeds between wet and dry samples. This technique allows for the study of molecular mobility *in vivo* in biological systems and can provide a spectrum of the spin probe from the cytoplasm. The rotational mobility may be used as a measure of the intracellular viscosity of the sample.

2. MATERIALS AND METHODS

2.1. Preparation of samples

Autumn sown facultative wheat (*cv.* Lennox) (winter wheat) was obtained from the Department of Agroecology and Plant Production at the University of Agriculture in Kraków. The seeds were stored at room temperature with a hydration level of $\Delta m/m_0 = 0.095 \pm 0.002$, where m_0 is the dry mass of the thallus and Δm is the mass of water taken up from the gaseous phase. Prior to the hydration experiment, air-dried samples were incubated for 558 h over silica gel ($p/p_0 = 0\%$) and dehydrated to $\Delta m/m_0 = 0.036 \pm 0.001$. The gaseous phase hydration courses of the samples were measured at room temperature ($t = 22°C$), over the surfaces of the saturated solutions: LiCl ($p/p_0 = 11\%$), CH$_3$COOK ($p/p_0 = 23\%$), CaCl$_2$ ($p/p_0 = 32\%$), Mg(NO$_3$)$_2$ ($p/p_0 = 53\%$), NH$_4$NO$_3$ ($p/p_0 = 63\%$), Na$_2$S$_2$O$_3$ ($p/p_0 = 76\%$), Na$_2$SO$_4$ ($p/p_0 = 93\%$), K$_2$SO$_4$ ($p/p_0 = 97\%$), and over the surface of water ($p/p_0 = 100\%$) for 686 h. The dry mass of the seeds was determined after heating at 70°C for 162 h.

The basic geometric dimensions of the seeds, such as their length (largest dimension), width (medium dimension) as well as thickness were determined using an electronic digital micrometer (Edkar, Poland) having a least count of 0.001 mm. The seed mass was determined to the nearest 0.1 mg using a WAS 220/X laboratory weighing scale. The grains were previously selected to exclude damaged grains before the experimental measurements were conducted.

The physical properties of the analysed seeds are presented in Table 1. The average mass of the wheat seed was 49.90 mg, with a length of 6.53 mm, a width of 3.46 mm, and a thickness of 3.08 mm.

Table 1. Statistical characteristics of the physical parameters of wheat seeds

Physical parameter	Minimum	Maximum	Average
Mass (mg)	33.9	65.2	49.90 ± 6.90
Length (mm)	5.93	7.22	6.53 ± 0.30
Thickness (mm)	3.04	3.97	3.08 ± 0.21
Width (mm)	2.13	3.53	3.46 ± 0.17

2.2. Statistical analysis

An analysis of the mathematical models was performed using Origin 2019 software. A chi-squared goodness of all of the tested fits was performed separately. The best fit procedure was determined together with the calculations of the values of the appropriate coefficients. The significance level for all of the tests was p < 0.05 (F-test).

2.3. Hydration kinetics

The hydration courses were fitted well using the following one-exponential function:

$$\Delta m/m_0 = A_0 + A_1 \left[1 - exp \left(-\frac{t}{t_1} \right) \right], \tag{1}$$

where: $\Delta m/m_0$ is the relative mass increase, A_0 is the saturation hydration level for the fraction of very tightly bound water not removed by incubation over silica gel ($p/p_0 = 0\%$), A_1 is the saturation hydration level for the fraction of tightly bound water, and t_1 is the hydration time.

2.4. Dent model

The total saturation hydration level, C_h, was calculated as the sum of both saturation hydration components:

$$C_h = A_0 + A_1. \tag{2}$$

The Dent's model is a multilayer sorption model that distinguishes between two types of water binding sites: (i) "primary" water binding sites, directly bound to the adsorbent surface, and (ii) "secondary" water binding sites, bound to primary and further bound water molecules.

The sorption isotherm for the Dent's model can be described by the following equation:

$$\frac{\Delta m}{m_0} = C_h(h) = \frac{\Delta M}{m_0} \frac{b_1 h}{(1-bh)(1+b_1 h - bh)}, \tag{3}$$

where: h is the relative humidity (p/p_0) expressed in absolute units and $\Delta M/m_0$ is the mass of water saturated primary water binding sites. If the number of primary water binding sites occupied by i water molecules is S_i and the contribution of empty primary water binding sites is equal to S_0, then $S_0/S_1 = 1/b_1$. For the Dent's model the sorption isotherm approximates the population of subsequent layers of the secondary bound water fraction in different ways, $S_{n+1}/S_n|_{h=1}$, is different from the BET (Brunauer – Emmet -Teller) model, for which $b = S_{n+1}/S_n|_{h=1} = 1$ (Brunauer *et al.*, 1938). For the Dent's model, this number varies to some extent between 0 and 1, thereby simulating the effect of clustering. Equation (3) can also be rewritten in a parabolic form (Eq. 5). Both forms give us the values of the parameters: $\frac{\Delta M}{m_0}$, b_1, b (Harańczyk *et al.*, 2008; 2009a, b). The parameters of the Dent model are related to those of the GAB model:

$$b = k, \tag{4a}$$

$$b_1 = CK, \tag{4b}$$

$$w_m = \frac{\Delta M}{m_0}, \tag{4c}$$

$$a_w = h, \tag{4d}$$

where: a_w is the water activity, this is related to the relative humidity ($h = p/p_0$), w_m is the moisture content (GAB model) corresponding to the water monolayer of the sample surface (Dent model), and the parameters K and C characterize the sorption properties of the substance (Blahovec and Yanniotis, 2008).

Another form of Eq. (3), which is used to calculate the parameters $\frac{\Delta M}{m_0}$, b_1 and b, is Eq. (5):

$$\frac{h}{\Delta m/m_0} = A + Bh + Ch^2, \quad (5)$$

where:

$$A = \frac{1}{\Delta M/m_0 \, b_1}, \quad (5a)$$

$$B = \frac{b_1 - 2b}{\Delta M/m_0 \, b_1}, \quad (5b)$$

$$C = \frac{b^2 - bb_1}{\Delta M/m_0 b_1}. \quad (5c)$$

The parameters A, B, and C are calculated from the parabolic Eq. (5) using regression analysis. The Dent's parameters are related to the parabola parameters by equations:

$$b = \frac{\sqrt{B^2 - 4AC} - B}{2A}, \quad (5d)$$

$$\frac{\Delta M}{m_0} = \frac{1}{A \, b_1}, \quad (5e)$$

$$b_1 = \frac{B}{A} + 2b. \quad (5f)$$

In more complex biological systems, *e.g.*, seeds, there is a problem with the correct approximation of sorption data using the Dent model. For this reason, the generalized Dent model, analogous to the generalized GAB model has been proposed (Blahovec and Yanniotis, 2008).

2.5. Generalized model

Equation 5, written with the standard Dent model parameters, gives the following equation:

$$\frac{h}{\Delta m/m_0} = \frac{1}{\Delta M/m_0 b_1} + \frac{(b_1 - 2b)}{\Delta M/m_0 b_1} h + \frac{(b^2 - bb_1)}{\Delta M/m_0 b_1} h^2. \quad (6af)$$

For $b_1 = Cb$, we obtain:

$$\frac{h}{\Delta m/m_0} = \frac{1}{\Delta M/m_0 Cb} + \frac{(C-2)}{\Delta M/m_0 C} h + \frac{b(1-C)}{\Delta M/m_0 C} h^2. \quad (6b)$$

The generalization of the Dent sorption isotherm is based on the assumption that the parameter $C = b_1/b$ is not a constant but rather depends on relative humidity and can be expressed in the form:

$$\frac{1}{C} = \frac{1}{C_0}(1 + x_1 h + x_2 h^2 + \cdots). \quad (7)$$

The combination of Eqs (6b) and (7) gives the generalized Dent model. The formulas for calculating the parameters C_0, b, b_1, $\frac{\Delta M}{m_0}$, for different polynomial orders (from the third to the sixth) are given in Table 2.

For the third and fourth orders, Eq. (5) can be rewritten as follows:

$$\frac{h}{\Delta m/m_0} = A' + B'h + C'h^2 + D'h^3, \quad (8a)$$

$$\frac{h}{\Delta m/m_0} = A'' + B''h + C''h^2 + D''h^3 + E''h^4. \quad (8b)$$

2.6. ^{1}H-NMR experimental parameters

The ^{1}H-NMR free induction decay (*FID*) measurements were conducted using a high-power WNS HB-65 NMR relaxometer constructed by Waterloo NMR Spectrometers (Waterloo, Ontario, Canada). The resonance frequency was

Table 2. Calculation of the parameters x_i, $\Delta M/m_0$, C_0, b, b_1

Third order	Fourth order	Fifth order	Sixth order
$x_1 = \dfrac{D}{Ab^2}$	$x_1 = \dfrac{1}{Ab^2}(D + 2Abx_2)$	$x_1 = \dfrac{1}{Ab^2}(D + 2Abx_2 - Ax_3)$	$x_1 = \dfrac{1}{Ab^2}(D + 2Abx_2 - Ax_3)$
$\dfrac{\Delta M}{m_0} = \dfrac{1}{B + A(2b - x_1)}$	$x_2 = \dfrac{E}{Ab^2}$	$x_2 = \dfrac{E}{Ab^2} + \dfrac{2x_3}{b}$	$x_2 = \dfrac{E}{Ab^2} + \dfrac{2x_3}{b} - \dfrac{x_4}{b^2}$
$C_0 = \dfrac{1}{A\dfrac{\Delta M}{m_0}b}$	$\dfrac{\Delta M}{m_0} = \dfrac{1}{B + A(2b - x_1)}$	$x_3 = \dfrac{F}{Ab^2}$	$x_3 = \dfrac{F}{Ab^2} + \dfrac{2x_4}{b}$
$b_1 = b \, c_0$	$C_0 = \dfrac{1}{A\dfrac{\Delta M}{m_0}b}$	$\dfrac{\Delta M}{m_0} = \dfrac{1}{B + A(2b - x_1)}$	$x_4 = \dfrac{G}{Ab^2}$
	$b_1 = b \, c_0$	$C_0 = \dfrac{1}{A\dfrac{\Delta M}{m_0}b}$	$\dfrac{\Delta M}{m_0} = \dfrac{1}{B + A(2b - x_1)}$
		$b_1 = b \, c_0$	$C_0 = \dfrac{1}{A\dfrac{\Delta M}{m_0}b}$
			$b_1 = b \, c_0$

30 MHz, the main static magnetic field was $B_0 = 0.7$ T, the transmitter power was 400 W, the length of the $\pi/2$ pulse was 1.5 μs, and the repetition time was 2 s. The data were averaged over 1000 accumulations and analysed using the CracSpin programme (Węglarz and Harańczyk, 2000).

2.7. ¹H-NMR free induction decays (*FIDs*) measurements

¹H-NMR *FID*s were recorded at room temperature for *Triticum aestivum,* L. seeds hydrated to $\Delta m/m_0 = 0.0421$; 0.0446; 0.0488; 0.128; 0.229 and to 0.396. The recorded *FID*s were fitted using two models.

The first fitted model was a superposition of the Gaussian component S and two exponentially relaxing components L_1 and L_2 :

$$FID(t) = S \exp\left(-\left(\frac{t}{T_{2S}^*}\right)^2\right) + L_1 exp\left(-\frac{t}{T_{2L1}^*}\right) + L_2 exp\left(-\frac{t}{T_{2L2}^*}\right). \quad (9)$$

where: T_{2S}^* is the proton spin-spin relaxation time for the solid component S, which is defined as the time required for the Gaussian function to decay to 1/e of its initial amplitude, whereas T_{2L1}^* is the effective spin-spin relaxation time of the tightly bound water fraction (L_1), and T_{2L2}^* is the effective spin-spin relaxation time of the loosely bound water fraction (L_2). The spin-spin relaxation times were shortened by B_0 inhomogeneities (Chavhan *et al.*, 2009).

The *FID* function may be expanded by a series of moments M_n (Abragam, 1983):

$$F(t) = \sum_{n=0}^{\infty} M_{2n} \frac{(-1)^n t^{2n}}{(2n)!} = 1 - \frac{M_2 t^2}{2!} + \frac{M_4 t^4}{4!} - \frac{M_6 t^6}{6!} + \cdots. \quad (10)$$

The equation above resembles a function which is a product of the sine function and the Gaussian function (in the NMR community this is often called an Abragam function):

$$F_s(t) = \sum_{n=0}^{\infty} \exp(-\frac{1}{2}a^2 t^2)\frac{sinbt}{bt}, \quad (11)$$

which can be expanded into a series:

$$F_s(t) = 1 - \left(a^2 + \frac{1}{3}b^2\right)\frac{t^2}{2!} + \left(3a^4 + 2a^2 b^2 + \frac{1}{5}b^4\right)\frac{t^4}{4!} - \cdots. \quad (12)$$

For the second and fourth moments, there are:

$$M_2 = a^2 + \frac{1}{3}b^2, \quad (13)$$

$$M_4 = 3a^4 + 2a^2 b^2 + \frac{1}{5}b^4. \quad (14)$$

The second model is often used to describe the carbohydrate systems in a glassy state and includes the superposition of the sinc function multiplied by the Gaussian function, as well as two exponential components:

$$FID(t) = S \exp\left(-\left(\frac{t}{T_{2S}^*}\right)^2\right)\frac{sin(bt)}{bt} + L_1 exp\left(-\frac{t}{T_{2L1}^*}\right) + L_2 exp\left(-\frac{t}{T_{2L2}^*}\right). \quad (15)$$

This Abragam function (Eq. (15)) often better fits the proton *FID* signal in many low-mobility systems in a glassy state (Van den Dries *et al.*, 1998). For $b \rightarrow 0$, we obtain:

$$\lim_{b \to 0} \frac{sin(bt)}{bt} = 1. \quad (15a)$$

A comparison between these two models was made using the least-square deviation χ^2, defined by:

$$\chi^2 = \frac{1}{N}\sum_i (S_i - F_i)^2 , \quad (15a)$$

where: S_i and F_i are the experimental and calculated data points, and N is the number of data points.

3. RESULTS

3.1. Hydration kinetics

Figure 1 shows the hydration courses for the winter wheat *Triticum aestivum,* L. seeds, performed using the gaseous phase. The relative mass increase, $\Delta m/m_0$, was registered. The courses, which were carried out at a relative humidity p/p_0 ranging from 11 to 100% were well-fitted using a single exponential function. Table 3 presents the coefficients for the exponential model of the moisture content achieved during hydration from the gaseous phase, at different humidity levels of the sample. The hydration kinetics allowed us to determine two fractions of bound water: (i) a fraction of very tightly bound water, with an average value $A_0^h = 0.082 \pm 0.016$ over all hydration courses, and (ii) a fraction of tightly bound water, with $A_1^h = 0.048 \pm 0.033$ and a hydration time of $t_1^h = (62 \pm 23)$ h.
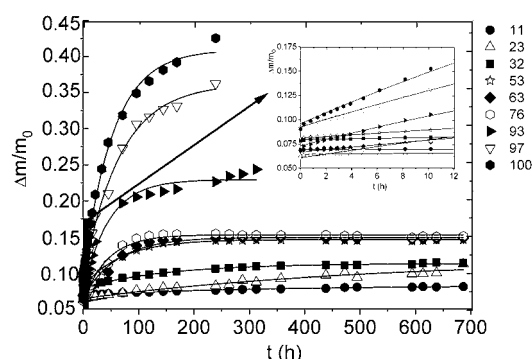

Fig. 1. Hydration kinetics of the winter wheat *Triticum aestivum,* L, recorded as the relative mass increase expressed in units of dry mass, $\Delta m/m_0$. The hydration was performed from the gaseous phase at different values of relative humidity p/p_0. Target humidity p/p_0: 11% – closed circles, 23% – open triangles, 32% closed squares, 53% – open stars, 63% – closed diamonds, 76% – open hexagons, 93% – closed triangles, 97% – open triangles, 100% – closed hexagons. The errors are within the plot symbols.

3.2. Sorption isotherm

Figure 2 shows the parabolic form of the sorption isotherm for *Triticum aestivum,* L. seeds. The data were obtained from the hydration kinetics values attained at room temperature. As shown in Fig. 3, the sorption isotherm has a sigmoidal form. The generalized Dent's model

Ta b l e 3. Coefficients of the exponential model of the moisture content of wheat seeds during hydration from the gaseous phase at different humidity levels of the sample

Relative humidity	A_0	A_1	$t_1(h^{-1})$	R^2	$\chi^2 \times 10^{-5}$
11	0.06936 ± 0.00051	0.01308 ± 0.00035	326 ± 19	0.996	0.0272
23	0.0644 ± 0.0089	0.05500 ± 0.0062	500 ± 100	0.978	15.5
32	0.07952 ± 0.00041	0.03366 ± 0.00030	155.50 ± 4.4	0.998	1.13
53	0.08074 ± 0.00069	0.06532 ± 0.00055	68.60 ± 2.1	0.998	6.08
63	0.0666 ± 0.0014	0.08260 ± 0.0011	61.70 ± 3.3	0.994	24.6
76	0.0608 ± 0.0013	0.09210 ± 0.0010	44.11 ± 2.0	0.996	20.38
93	0.0732 ± 0.0039	0.15630 ± 0.0029	45.80 ± 3.6	0.993	86.2
97	0.0925 ± 0.0076	0.26970 ± 0.0052	66.90 ± 3.8	0.997	66.1
100	0.0959 ± 0.0066	0.31370 ± 0.0046	54.00 ± 2.4	0.997	85.1
Average	0.082 ± 0.016	0.04800 ± 0.033	62.0 ± 23	–	–
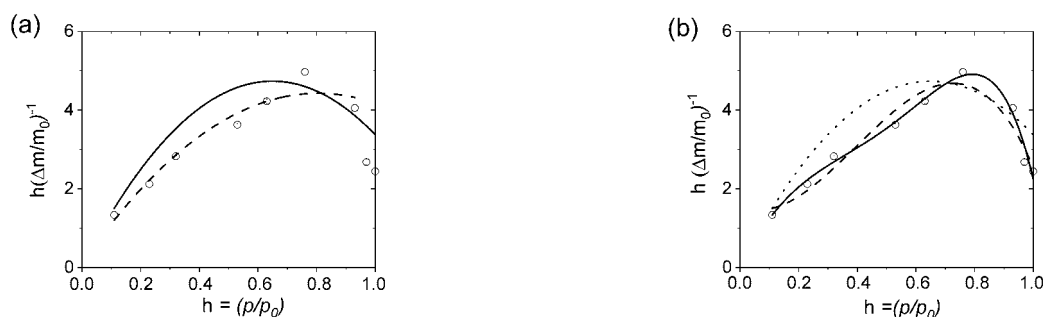
Fig. 2. Parabolic form of the sorption isotherm for winter wheat *Triticum aestivum*, L.: a) open circles – experimental data; dashed line – Dent model fitted to part of the experimental data (from $h = 0.11$ to $h = 0.93$); black line – Dent model fitted to all of the experimental data (from $h = 0.11$ to $h = 1$); b) open circles – experimental data, dotted line – Dent model fitted to all of the experimental points, dashed line – the polynomial of the fourth order, solid line – the polynomial of the sixth order.
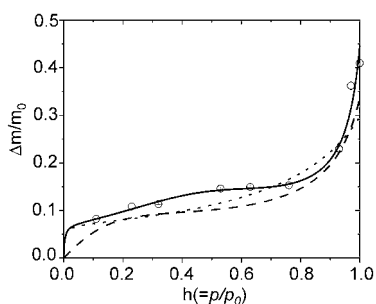
Fig. 3. Sorption isotherm for winter wheat *Triticum aestivum*, L. (open circles – experimental data; dotted line – Dent model fitted to the experimental data; dashed line – the polynomial of the third order; solid line – the polynomial of the sixth order).

fits the data better than the Dent's model (Dent, 1977). The experimental data points were initially fitted using the standard Dent's model at relative humidity values ranging from $h = 0.11$ up to $h = 1$. However, this model was found to be insufficient ($R^2 = 0.627$). In order to improve the fit, we applied the model to the data between the relative humidities $h = 0.11$ and 0.93, resulting in a better R^2 value

of 0.949. Increasing the polynomial order further improved the fit, with the third-order polynomial having an R^2 value of 0.922, and the sixth-order polynomial having an R^2 value of 0.974 (Table 4).

Figure 2b shows the higher-order polynomials that were fitted to the experimental points. As the polynomial order (Eq. (5)) increases, parameter b rises from $b = 0.768$ to $b = 0.95$ for the fifth-order polynomial (Table 5). Subsequently, a small decline in b was noted for the sixth-order polynomial ($b = 0.947$). The water content of the primary binding sites ($\Delta M/m_0$) decreased slightly with increasing polynomial order, from $\Delta M/m_0 = 0.0689$ (2nd order) to $\Delta M/m_0 = 0.0197$ (5-th order), except for the sixth-order polynomial, which showed a slight increase ($\Delta M/m_0 = 0.0209$).

3.3. ¹H-NMR measurements

The proton free induction decay (*FID*) signals recorded for the *Triticum aestivum,* L. wheat seeds which were fitted according to the models from Eqs (9) and (15) are shown in Fig. 4a. Figure 4b shows the FID signals recorded in the first 180 µs. A better fit, especially for the lower hydration

Ta ble 4. R^2 values for the Dent's and generalized Dent's models, using polynomials from the third to the sixth orders for winter wheat seed

Polynomial degree	Order					
	Second (fitted up to $h = 1$)	Second (fitted up to $h = 0.93$)	Third	Fourth	Fifth	Sixth
A	0.05	0.0980	1.56	0.098	0.3103	0.05
B	14.43	10.76	-3.21	17.04	9.69	13.89
C	-11.11	-6.66	26.61	-52.03	0.08698	-19.59
D	0	0	-22.42	89.66	-47.87	-15.970
E	0	0	0	-52.47	99.92	91.14
F	0	0	0	0	-59.93	-82.74
G	0	0	0	0	0	14.68
R^2	0.6269	0.9492	0.9220	0.9698	0.9729	0.9741

Ta ble 5. Parameters of the Dent model and the generalized Dent model for winter wheat seeds

Polynomial degree	2 – Dent model		3	4	5	6
	fitted up to $h = 1$	fitted up to $h = 0.93$				
b	0.768	0.618	0.897	0.938	0.950	0.947
b_1	290.12	110.98	20.17	43.3111	164.02	957.85
$\Delta M/m_0$	0.0689	0.0919	0.0317	0.0236	0.0197	0.0209
C_0	377.81	179.61	22.48	46.17	164.02	1011.68
x_1	–	–	-17.80	-257.38	-130.92	-30.41
x_2	–	–	–	-608.35	-93.57	-770.27
x_3	–	–	–	–	-213.89	-1154.4
x_4	–	–	–	–	–	327.48
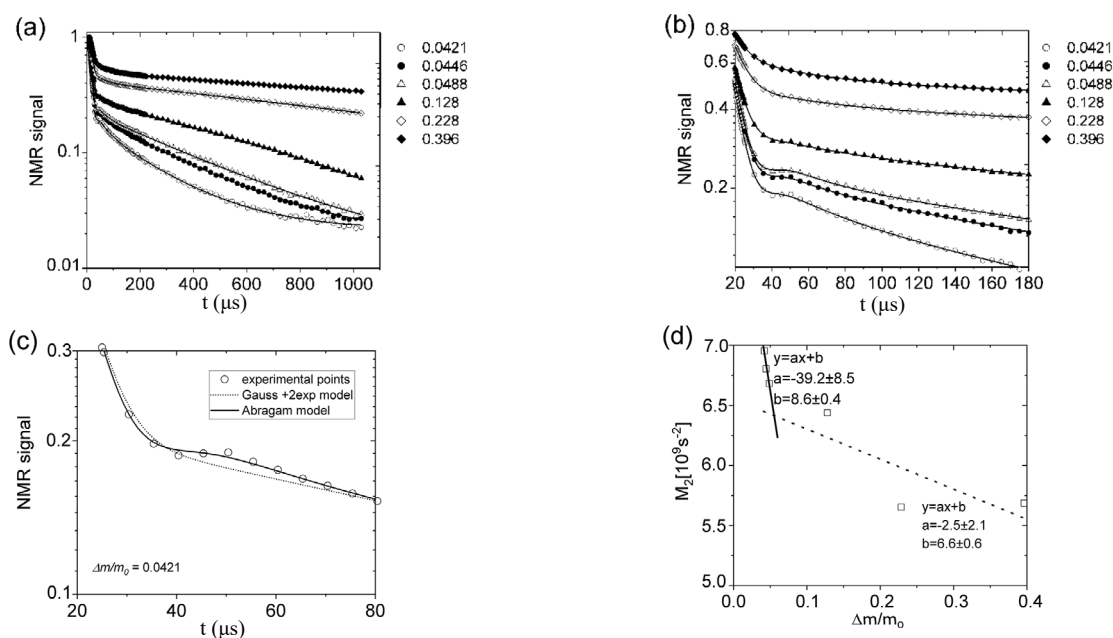
Fig. 4. *FID* signals recorded at room temperature for *Triticum aestivum*, L. wheat seeds: a) at different hydration levels of the samples; b) *FID* signals recorded in the first 180 µs; c) comparison of two models fitted to the *FID* signal, recorded at $\Delta m/m_0 = 0.0421$. Solid line – Abragam model (Eq. (15)); dotted line – superposition of the Gauss model and two exponents (Eq. (9)); d) effect of water on the second moment for wheat seed at 25°C.
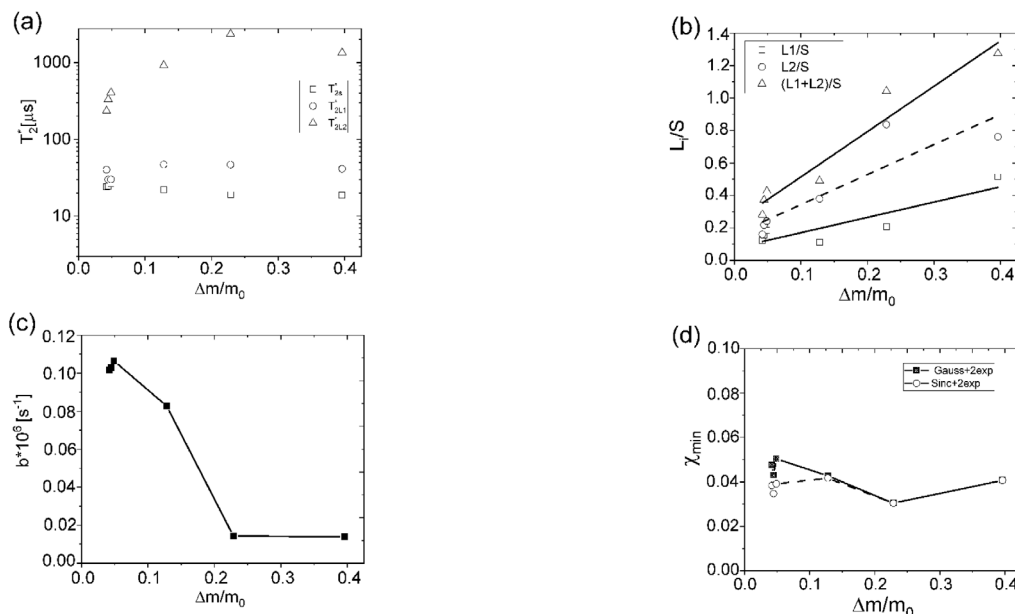
Fig. 5. Hydration dependence of NMR relaxation parameters in the Abragam model (Eq. (15)) for a sample of *Triticum aestivum,* L. seeds measured at the room temperature: a) T_2^* Solid Gaussian component (S) = open squares, tightly bound water fraction (L_1) = open circles, loosely bound water fraction (L_2) = open triangles; b) L_i/S; c) b parameter from Eq. (15); and d) plot resulting from the fitting of the models described by Eq. (9) (solid squares and solid line) and Eq. (5) (open circles and dashed line).

levels of the sample (up to $\Delta m/m_0 = 0.128$), was obtained using Eq. (15), where the solid-like proton fraction was fitted using the Abragam function, whereas the liquid-like proton fraction is accounted for by applying the two-exponential function with relaxation times T_{2L1}^* and T_{2L2}^*. Figure 4d shows the effect of water on M_2, at 25°C. As the hydration level increases, a decrease in M_2 was observed, this suggests the decreasing strength of the dipolar interactions associated with the increasing mobility of the rigid protons.

Figures 5a-c show the dependence of the NMR relaxation parameters on the hydration level of the sample, recorded at room temperature, for the model described by Eq. (15). Figure 5a shows the relaxation times recorded for the sample. The shortest values of relaxation time were recorded for protons, which build up in the solid matrix of the sample and had averaged values of spin-spin relaxation time equal to $T_{2s}^* \approx 22\mu s$. The signal originating from the mobile protons was fitted by a two-exponential function over a wide range of the sample hydration level. For the mobile proton fraction L_1 the value of the effective spin-spin relaxation time did not depend to a substantial extent on the hydration level of the sample (Fig. 5a) and its averaged value was equal to $T_{2L1}^* \approx 39\mu s$. An L_2 signal component with a longer spin-spin relaxation time and an average value of $T_{2L2}^* \approx 930\mu s$ was detected across all hydration levels (Fig. 5b). The amplitude of both mobile proton signal components (L_1 and L_2), expressed in units of solid signal amplitude L_1/S and L_2/S, linearly increased with increasing sample hydration levels:

$$L_1/S(\Delta m/m_0) = (0.94 \pm 0.25) + (0.076 \pm 0.048) \tag{17a}$$

$$L_2/S(\Delta m/m_0) = (1.85 \pm 0.47) + (0.159 \pm 0.093) \tag{17b}$$

In Figure 5c, the value of the b parameter of the Abragam model decreases to a significant extent as the hydration level varies from $\Delta m/m_0 = 0.086$ to $\Delta m/m_0 = 0.229$. Figure 5d compares the minimal values of χ_{min} for the models described by Eqs (9) and (15) as a function of the total hydration level. For higher hydration levels of the sample (from $\Delta m/m_0 = 0.128$ up to $\Delta m/m_0 = 0.396$), both models yield similar values of χ_{min}. However, for lower levels of hydration (up to $\Delta m/m_0 = 0.128$), a better fit was obtained by using Eq. (15), this was confirmed by lower values of χ_{min}.

4. DISCUSSION

The hydration kinetics results suggest that the amount of very tightly bound water ($A_0^h = 0.082 \pm 0.016$) was comparable, but slightly higher than those of Antarctic lichens such as *Umbilicaria aprina* ($A_0^h = 0.054$) or *Usnea antarctica* Du Rietz, ($A_0^h = 0.040$). The hydration process of wheat seeds was considerably slower than that of lichens, with a hydration constant of $t_1^h = (62 \pm 23)\ h$. For example, Bacior *et al.* (2017) found that the thallus of *T. complicatulum* had a tightly bound water hydration time of $t_1^h = 1.45$ h, while the Antarctic alga *Prasiola crispa* had a hydration time of $t_1^h = 0.37$ h. This difference may be attributed to the compact structure of the seed, which slows down the hydration process, in contrast to the lichen and alga thalli with their loosely packed cells. The binding strengths of the two fractions of water bound in wheat seeds differ depending on their proximity to the seed surfaces. Harańczyk *et al.* (1996) also revealed a single-exponential pattern in

the hydration process of wheat seed "Jara". The hydration process was described for seeds soaked between two layers of blotting paper, for seeds immersed in water, or for seeds hydrated over the water surface. The study analysed the hydration process during the first six hours of water adsorption, without prior dehydration over silica gel. A one-exponential process of hydration was also observed in freeze-dried model membranes (Harańczyk *et al.*, 2009a).

A sorption isotherm provides the parameter $b = 0.947$, which indicates the population of subsequent layers of secondary bound water fractions ($b = S_{n+1}/S_n|_{h=1}$). This parameter closely matches the values obtained for the Antarctic lichen *Turgidosculum complicatulum* ($b = 0.958$) and the alga *Prasiola crispa* ($b = 0.874$) (Bacior *et al.*, 2017). Additionally, it is similar to the value observed for DNA-DDCA complexes, ($b = 0.932$) (Harańczyk *et al.*, 2013).

The hydration kinetics indicate that the amount of very tightly bound water ($A_0 = 0.082$) exceeds the value expected for a monolayer on the wheat grain surface ($\Delta M/m_0 = 0.0209$), this suggests that only a portion of this fraction constitutes the monolayer. The mass of water saturating primary water-binding sites is lower than that for lichenized fungal species. For example, *Turgidosculum complicatulum* has a value of $\Delta M/m_0 = 0.055$, whereas for the foliose thalli of *Umbilicaria aprina* $\Delta M/m_0 = 0.054$, and for Antarctic alga *Prasiola crispa*, $\Delta M/m_0 = 0.131$ (Bacior *et al.*, 2017; Harańczyk *et al.*, 2008). At $h = 1$, the fraction of unoccupied primary water binding sites for *Triticum aestivum,* L. seeds is $1/b_1 = 0.104\%$. This value is higher than that observed for some species of lichens, *e.g.* for *U. aprina*, where $1/b_1 = 0.02\%$ (Harańczyk *et al.*, 2008). This suggests that the wheat seed surfaces may be less hydrophilic than those of Antarctic lichens.

For samples with higher hydration levels ($\Delta m/m_0 > 0.128$), the NMR signal was properly described using a Gaussian function and two exponents (Eq. (9)). This approach has been shown to effectively describe *FID* signals in biological systems, these include Antarctic lichens or algae (Bacior *et al.*, 2017, 2019, 2022), freeze-dried dipalmitoylphosphatidylcholine (DPPC) multilamellar membranes (Harańczyk *et al.*, 2016), lyophilized photosynthetic lamellae (Harańczyk *et al.*, 2015) or didecyldimethylammonium chloride modified DNA (Harańczyk *et al.*, 2013). However, the model did not successfully fit the shape of the *FID* function for the dry wheat seed ($\Delta m/m_0 < 0.128$), particularly in the initial 80 μs of the NMR *FID* signal (Fig. 4c). The Abragam function was used to fit the *FID* signal for these dry samples, as has been done in several other systems, such as maltose with water (van den Dries *et al.*, 1998), starch mixed with sucrose (Roudaut *et al.*, 2009), amylose films with glycerol (Partanen *et al.*, 2004), and Antarctic lichen *U. aprina* (Harańczyk *et al.*, 2008), where despite the presence of this function, the glassy state was not confirmed by the DSC measurements.

The M_2 values for all of the hydration levels of the samples range from 5.7×10^9 to 7.0×10^9 s^{-2}, which is consistent with the values predicted by Partanen *et al.* (2004) for amylose-glycerol-water and Roudaut *et al.* (2009) for gelatinized starch and also for samples consisting of 20% sucrose and starch. The decrease in M_2 values was more pronounced for the more dehydrated samples, up to $\Delta m/m_0 = 0.049$, with a slope of the line equal to a = -39.2. The decrease was less pronounced for the more hydrated samples, with a slope of the line equal to a = -2.5. Conversely, for the maltose-water samples, a higher slope of the second moment (M_2) was observed for higher temperatures of the sample (van der Dries *et al.*, 1998).

The spin-spin relaxation time of the solid proton fraction L_1 ($T_{2s}^* \approx 22$ μs) was similar to that of lichens. For example, *T. complicatulum* thallus produced a value of ($T_{2s}^* \approx 18$ μs), which is also similar to other biological systems such as photosynthetic membranes (Harańczyk *et al.*, 2009). However, the spin-spin relaxation time ($T_{2L1}^* \approx 39$ μs) for the mobile proton fraction L_1 (Fig. 5a) is shorter than that observed for DNA-DDCA complexes ($T_{2L1}^* \approx 80$ μs) (Harańczyk *et al.*, 2013) or for Antarctic lichens, such as *Umbilicaria aprina*, *Turgidosculum complicatulum* ($T_{2L1}^* \approx 71$ μs), *Umbilicaria antarctica* and *Niebla tigrina* from Atacama Desert ($T_{2L1}^* \approx 100$ μs) (Harańczyk *et al.*, 2008; Bacior *et al.*, 2017; Harańczyk *et al.*, 2021). These findings suggest that the tightly bound water fraction in *Triticum aestivum,* L. seeds may have less mobility due to the different microstructure of the sample, which has smaller pores as compared to those of lichens or algal thalli.

The value of the spin-spin relaxation time for the L_2 signal component ($T_{2L2}^* \approx 930$ μs) is similar to that observed for Antarctic lichen *U. antarctica*, *N. tigrina*, as well as for the didecyldimethylammonium chloride DNA complex ($T_{2L2}^* \approx 1000$ μs) (Harańczyk *et al.*, 2008, 2013, 2021). The spin-spin relaxation time increased as the sample became more hydrated, from a value of $T_{2L2}^* \approx 234$ μs for the driest sample ($\Delta m/m_0 = 0.0421$), to a value of $T_{2L2}^* \approx 1341$ μs for the most hydrated sample ($\Delta m/m_0 = 0.396$).

Wheat seeds, like other orthodox seeds, can survive deep dehydration due to the accumulation of substances that enhance drought resistance, such as sugars, polyols, amino acids, and LEA proteins (Colville, 2017). These biological systems maintain a high degree of stability and a low degree of molecular mobility above the glass transition temperature. This ecological advantage ensures seed stability under unfavourable conditions of temperature or water content which cause tissues to exit the glassy state (Buitink and Leprince, 2008). At 20°C and 50% of RH, the seed's matrix is close to its glass transition temperature Tg. The rotational mobility of the pea (*Pisum sativum* L.) axes was measured during dehydration at room temperature and below 0.8 g H_2O g^{-1} DW revealed that the cytoplasm had become highly viscous. During drying below 0.3g H_2O g^{-1} DW, the molecular mobility of the cytoplasm decreased by

five orders of magnitude. At approximately 0.1 g H_2O g^{-1} DW, the cytoplasm vitrified and became glassy. Glass formation has also been observed in pollen and in the resurrection plant *Craterostigma plantagineum* (Buitink and Leprince, 2008). The role of glasses in seeds is crucial as they prevent conformational changes in proteins and increase the stability of enzymes (Chang *et al.*, 1996; Prestrelski *et al.*, 1993). Golovina *et al.* (1997) and Buitink *et al.* (1998) found that wheat (*Triticum* spp.) seeds presented no evidence of protein denaturation after 28 years of dry storage when the seeds were in a glassy state. Seed deterioration was accelerated when the seeds were not in a glassy state. During the dehydration process in seeds, when the relative humidity (RH) is lower than 90%, the hydrated cytoplasm becomes more viscous and causes the dry components of the cells to squeeze together. At RH values between 50 and 25%, cytoplasm solidifies and turns into glass (Nadarajan *et al.*, 2023).

These findings are consistent with the results obtained. The values of the nuclear spin-spin relaxation time T_{2L1}^* did not change significantly with the hydration level of the sample, particularly for hydration levels higher than $\Delta m/m_0$ = 0.128, which is a critical value in the changes in the FID signal, this is possibly related to the glass transition. Above the glass transition temperature, the cytoplasm of desiccation-tolerant organisms remains quite immobile (Vertucci *et al.*, 1994). This suggests that the biological system is stable and exhibits a high viscosity ($>10^8$ Pa s). Buitink *et al.* (2000) discovered two phase transitions. The first transition is associated with the melting of the glassy state, while the second transition is linked to the critical temperature T_c. At this temperature, a drastic change in molecular dynamics occurs, this includes a shift from a solid-like to a liquid-like state. At this point, a viscous solution behaves like a normal liquid, with diffusional motions dominating. It has been suggested that the critical temperature for biological samples is over 50°C higher than T_g. This is because no kinetic changes occur in rotational mobility during seed heating to 45°C above their T_g (Buitink and Leprince, 2008). Seeds dried at room temperature reach a water content of approximately 0.1 to 0.12 g H_2O g^{-1} DW at the point of glass transition (Buitink and Leprince, 2008).

Sugars exhibit a different behaviour, with an abrupt decrease in viscosity that could lead to crystallization or to collapse. If the intracellular glass consists solely of sucrose, a slight increase in relative humidity or temperature could cause the glass to exceed its glass transition temperature (T_c), thereby leading to phase separation and a loss of macromolecular function or its integrity. High T_c could provide a physiological advantage to biological systems. The mobile proton signal components show a linear relationship, thereby indicating that the amount of substances dissolving during the hydration process of the sample is too low to be detected. This occurs within the range of the hydration levels studied, from $\Delta m/m_0$ = 0.0768 up to $\Delta m/m_0$ = 0.4096.

Harańczyk *et al.* (1996) observed a different relationship, but only investigated a single seed. They found that the NMR signal as a function of hydration level was well-fitted by a rational function, thereby indicating the dissolution of certain substances present in the single seed. This effect was not observed by these authors, this was probably due to the averaging of the results from multiple seeds.

The decrease in the *b* parameter of the Abragam model (Fig. 5c) is associated with the narrower line of the NMR signal in the frequency domain. This suggests a decrease in proton density, as the *b* parameter is dependent on the distance between protons (Derbyshire *et al.*, 2004). As *b* approaches 0, the sine function transforms into a Gaussian function, thereby indicating a change in the seed structure and the absence of a glassy state. Therefore, the "standard" model, as described in Eq. (9), can be effectively applied to samples with $\Delta m/m_0 > 0.128$, these correspond to a relative humidity of $h = 36.4\%$ (Fig. 4). For t-lower hydration levels ($\Delta m/m_0 < 0.128$), Eq. (15) is more appropriate.

5. CONCLUSIONS

A one-exponential model was used to successfully fit the hydration kinetics of *Triticum aestivum,* L. seeds. The model distinguished between two fractions of bound water: a very tightly bound water fraction ($\Delta m/m_0 = 0.082 \pm 0.016$) that was not removed by dehydration over silica gel, and a tightly bound water fraction ($\Delta m/m_0 = 0.048 \pm 0.033$) with a hydration time of $t_1^h = (62 \pm 23)h$. These two water fractions differ in their binding strength to the seed surface.

The Dent generalized model was found to be more effective in describing the sorption isotherm over the whole range of relative humidity, as opposed to the standard Dent's equation which was only useful up to a humidity level of $h < 0.9$. The higher order polynomials (fourth to sixth) were found to provide a better description of the data ($R^2 = 0.970$ and $R^2 = 0.974$) as compared to the second order polynomial ($R^2 = 0.627$).

For dry samples with a hydration level of $\Delta m/m_0 < 0.128$, the proton *FID* signals were more accurately described by the superposition of the Abragam function and two exponents. However, for samples with a higher hydration level, the proton signal of the sample was sufficiently well described by the Gaussian function and two exponents. A two-exponential function successfully fitted the liquid signal, with an effective spin-spin relaxation time of $T_{2L1}^* \approx 39\,\mu s$ and $T_{2L2}^* \approx 930\,\mu s$ for the tightly and also for the loosely bound water fractions, respectively.

6. ACKNOWLEDGEMENTS

Conflicts of Interest: The Authors do not declare any conflict of interest.

7. REFERENCES

Abdel-Aal, E.M., Rabalski, I., 2008. Bioactive compounds and their antioxidant capacity in selected primitive and modern wheat species. Open Agric. J. 2, 7-14, https://doi.org/10.2174/1874331500802010007

Abragam, A., 1983. The principles of nuclear magnetism. Oxford University Press, Oxford, UK, p. 618.

Arthur, E., Tuller, M., Moldrup, P, de Jonge, L.W., 2015, Evaluation of theoretical and empirical water vapor sorption isotherm models for soils. Water Resour. Res. 55, 190-205. https://doi.org/10.1002/2015WR017681

Bacior, M., Nowak, P., Harańczyk, H., Patryas, S., Kijak, P., Ligęzowska, A., 2017. Extreme dehydration observed in Antarctic *Turgidosculum complicatulum* and in *Prasiola crispa*. Extremophiles 21, 331-343. https://doi.org/10.1007/s00792-016-0905-z

Bacior, M., Harańczyk, H., Nowak, P., Kijak, P., Marzec, M., Fitas, J., Olech, M.A., 2019. Low-temperature immobilization of water in Antarctic *Turgidosculum* and in *Prasiola crispa*. Part I. *Turgidosculum complicatulum*. Colloids Surf. B. 173, 869-875, https://doi.org/10.1016/j.colsurfb.2018.10.059

Bacior, M., Harańczyk, H., Nowak, P., Kijak, P., Marzec, J., Fitas, M., Olech, M.A., 2022. Low-temperature investigation of residual water bound in free-living Antarctic *Prasiola crispa*. Antarct. Sci. 34(5), 389-400. https://doi.org/ 10.1017/S0954102022000335

Bewley, D.J., Bradford, K.J., Hillorst, H.W.M., Nonogaki, H., 2013. Germination. In: Seeds Springer, New York, NY. https://doi.org/10.1007/978-1-4614-4693-4_4

Blahovec, J., Yanniotis, S., 2008. GAB generalized equation for sorption phenomena. Food Bioproc. Tech. 1, 82-90. https://doi.org/10.1007/s11947-007-0012-3

Bradford, K.J., Dahal P., Van Asbrouck, J., Kunusoth, K., Bello, P., Thompson, J., Wu, F., 2018. The dry chain: Reducing postharvest losses and improving food safety in humid climates. Trends Food Sci. Technol. 71, 84-93. https://doi.org/10.1016/j.tifs.2017.11.002

Brunauer, S., Emmett, P.H., Teller, E., 1938. Adsorption of gases in multimolecular layers. J. Am. Chem. Soc. 60, 309-319. http://dx.doi.org/10.1021/ja01269a023

Buitink, J., Leprince, O., 2008. Intracellular glasses and seed survival in the dry state. C. R. – Biol. 331, 788-795. https://doi.org/10.1016/j.crvi.2008.08.002

Casada, M.E., 2002. Moisture adsorption characteristics of wheat and barley. Trans ASAE 45 361-368. https://doi.org/10.13031/2013.8507

Chang, B.S., Beauvais, R.M., Dong, A., Carpenter, J.F., 1996. Physical factors affecting the storage stability of freeze-dried interleukin-1 receptor antagonist: glass transition and protein conformation. Arch. Biochem. Biophys. 331, 249-258. https://doi.org/10.1006/abbi.1996.0305

Chavhan, G.B., Babyn, P.S., Thomas, B., Shroff, M.M., Haacke E.M., 2009. Principles, techniques, and applications of T_2*-based MR imaging and its special applications. Radiograph. 29, 1433-1449.

Che Lah, N.H., Enshasy, H.A.E., Mediani, A., Azizan, K.A., Aizat, W.M., Tan, J.K., Afzan, A., Noor, N.M., Rohani, E.R., 2023. An insight into the behaviour of recalcitrant

seeds by understanding their molecular changes upon desiccation and low temperature. Agron. 13(8), 2099. https://doi.org/10.3390/agronomy13082099

Chen, Y., Li, C., Zhang, B., Yi, J., Yang, Y., Kong, C., Lei, C., Gong, M., 2019. The role of the late embryogenesis-abundant (LEA) protein family in development and the abiotic stress response: A Comprehensive Expression Analysis of Potato (*Solanum tuberosum*). Genes 10, 148. https://doi.org/10.3390/genes10020148

Colville, L., 2017. Seed Storage. In: Thomas B., Murray B.G., Murray D.J. (Eds), Encyclopaedia of Applied Plant Sciences. Elsevier, Oxford, UK.

Dent, R.W., 1977. A multilayer theory for gas sorption. Part I: sorption of a single gas. Text. Res. J. 47, 145-152, https://doi.org/10.1177/004051757704700213

Derbyshire, W., Van den Bosch, M., van Dusschoten, D., MacNaughtan, W., Farat, I.A., Hemminga, M.A., Mitchell, J.R., 2004. Fitting of the beat pattern observed in NMR free-induction decay signals of concentrated carbohydrate-water solutions. J. Magn. Reson. 168, 278-283, https://doi.org/10.1016/j.jmr.2004.03.013

Ellis, R.H., 2022. Invited Review: Seed ageing, survival and the improved seed viability equation; forty years on. Seed Sci. and Technol. 50, 1-20, https://doi.org/10.15258/sst.2022.50.1.s.01

Ellis, R.H., Hong, T.D., Roberts, E.H., Tao, K.L., 1990. Low moisture content limits to relations between seed longevity and moisture. Ann. Bot., 65, 493-504, https://doi.org/10.1093/oxfordjournals.aob.a087961

Ferreira, M.S.L., Martre, P., Mangavel, C., Girousse, C., Rosa, N.N., Samson, M.F., Morel, M.H., 2012. Physicochemical control of durum wheat grain filling and glutenin polymer assembly under different temperature regimes. J. Cereal Sci. 56, 58-66, https://doi.org/10.1016/j.jcs.2011.11.001

Golovina, E.A., Wolkers, W.F., Hoekstra, F.A., 1997. Long-term stability of protein secondary structure in dry seeds, Comp. Biochem. Physiol. 117A, 343-348.

Harańczyk, H., Strzałka, K., Jasiński, G., Mosna-Bojarska, K., 1996. The initial stages of wheat (*Triticum aestivum*, L.) seed imbibition as observed by proton nuclear magnetic relaxation. Colloids Surf. A: Physicochem. Eng. Asp. 115, 47-54.

Harańczyk, H., Bacior, M., Olech, M.A., 2008. Deep dehydration of *Umbilicaria aprina* thalli observed by proton NMR and sorption isotherm. Antarct. Sci. 20, 527-535, https://doi.org/10.1017/S0954102008001363

Harańczyk, H., Bacior, M., Jamróz, J., Jemioła-Rzemińska, M., Strzałka, K., 2009a. Rehydration of digalactosyldiacylglycerol model membrane lyophilizates observed by NMR and sorption isotherm. Acta Phys. Pol. A. 115, 521-525, https://doi.org/10.12693/APhysPolA.115.521

Harańczyk, H., Bacior, M., Jastrzębska, P., Olech, M.A., 2009b. Deep dehydration of Antarctic lichen *Leptogium puberulum* Hue observed by NMR and sorption isotherm. Acta Phys. Pol. A. 115, 516-520, https://doi.org/10.12693/APhysPolA.115.516

Harańczyk, H., Czak, J., Nowak, P., Nizioł, J., 2010. Initial phases of DNA rehydration by NMR and sorption isotherm. Acta Phys. Pol. A. 117, 397-402, https://doi.org/10.12693/APhysPolA.117.397

Harańczyk, H., Kobierski, J., Nizioł, J., Hebda, E., Pielichowski, J., Zalitacz, D., Marzec, M., El-Ghayoury, A., 2013. Mild

hydration of didecyldimethylammonium chloride modified DNA by [1]H-nuclear magnetic resonance and by sorption isotherm. J. Appl. Phys. 113, 044702, https://doi.org/10.1063/1.4789011

Harańczyk, H., Leja, A., Nowak, P., Baran, E., Strzałka, K., 2016. The effect of mild rehydration on freeze-dried dipalmitoylphosphatidylcholine (DPPC) multilamellar membranes as observed by proton NMR and sorption isotherm. Acta Phys. Pol. A. 129, 179-184, https://doi.org/ 10.12693/APhysPolA.129.179

Harrington, J.F., 1960. Thumb Rules of Drying Seeds. Crops Soils, 13, 16-17.

Harrington, J.F., 1972. Seed storage and longevity. In: Seed Biology III; Ed. T.T. Kozlowski, Seed Biology, Insects, and Seed Collection, Storage, Testing and Certification, Academic Press, New York, 145-245, https://doi.org/10.1016/B978-0-12-395605-7.50009-0

Lemmens, E., De Brier, N., Goos, P., Smolders, E., Delcour, J.A., 2019. Steeping and germination of wheat (*Triticum aestivum* L.). I. Unlocking the impact of phytate and cell wall hydrolysis on bio-accessibility of iron and zinc elements. J. Cereal Sci. 90, 102847, https://doi.org/10.1016/j.jcs.2019.102847

Leprince, O., Pellizzaro, A., Berriri, S., Buitink, J., 2017. Late seed maturation: Drying without dying. J. Exp. Bot. 68, 827-841, https://doi.org/10.1093/jxb/erw363

Mitura, K., Cacak-Pietrzak, G., Feledyn-Szewczyk, B., Szablewski, T., Studnicki, M., 2023. Yield and Grain Quality of Common Wheat (*Triticum aestivum* L.) Depending on the Different Farming Systems (Organic *vs.* Integrated *vs.* Conventional), Plants 12(5), 1022, https://doi.org/10.3390/plants12051022

Nadarajan, J., Walters, C.T., Pritchard, H., Ballesteros, D., Colville, L.P., 2023. Seed longevity-the evolution of knowledge and a conceptual framework. Plants 12(3), 471, https://doi.org/10.3390/plants12030471

Pammenter, N.W., Berjak, P., 2007. A review of recalcitrant seed physiology in relation to desiccation-tolerance mechanisms. Seed Sci. Res., 9, 13-37, https://doi.org/10.17/S0960258599000033

Parihar, S.S., Dadlani, M., Mukhopadhyay, D., Lal, S.K., 2016. Seed dormancy, germination and seed storage in henna (*Lawsonia inermis*). Indian J. Agric. Sci. 86, 1201-1207, https://doi.org/10.56093/ijas.v86i9.61520

Partanen, R., Marie, V., MacNaughtanb, W., Forssell, P., Farhat, I., 2004. ^{1}H NMR study of amylose films plasticised by glycerol and water. Carbohydr. Polym. 56, 147-155, https://doi.org/10.1016/j.carbpol.2004.01.001

Prestrelski, S.J., Tedeschi, N., Arakawa, T., Carpenter, J.F., 1993. Dehydration-induced conformational transitions in proteins and their inhibition by stabilizers, Biophys. J. 65, 661-671, https://doi.org/ 10.1016/s0006-3495(93)81120-2

Rockland L.B., Beuchat L.R., 1987. Water Activity: Theory and Applications to Food, Rockland L.B., Beuchated L.R. (Eds). New York, USA.

Roudaut, G., Farhat, I., Poirier-Brulez, F., Champion, D., 2009. Influence of water, temperature and sucrose on dynamics in glassy starch-based products studied by low field ^{1}H NMR, Carbohydr. Polym. 77, 489-495, https://doi.org/10.1016/j.carbpol.2009.01.029

Samapundo, S., Devlieghere, F., De Meulenaer, B., Debevere, J.M., 2007. Sorption isotherms and isosteric heats of sorption of whole yellow dent corn, J. Food Eng. 79, 168-175, https://doi.org/10.1016/j.jfoodeng.2006.01.040

Shewry, P.R., 2018. Do ancient types of wheat have health benefits compared with modern wheat? J. Cereal Sci. 79, 469-476, https://doi.org/10.1016/j.jcs.2017.11.010

Shewry, P.R., Hey, S., 2015. The contribution of wheat to human diet and health, Food Energy Secur. 4, 178-202, https://doi.org/ 10.1002/fes3.64

Slade, L., Levine, H., 1994. Water and the glass transition: dependence of the glass transition temperature on composition and chemical structure: special implications for flour functionality and cookie baking. J. Food Eng. 22, 143-188.

Solberg, S., Yndgaard, F., Andreasen, C., von Bothmer, R., Loskutov, I.G., Asdal, Å., 2020. Long-term storage and longevity of orthodox seeds: A Systematic Review. Front. Plant Sci. 11, 1007, https://doi.org/10.3389

Van den Dries, I.J., van Dusschoten, D., Hemminga, A., 1998. Mobility in maltose-water glasses studied with ^{1}H NMR. J. Phys. Chem. B 102, 10483-10489.

Vertucci, C.W., Roos, E.E., 1990. Theoretical Basis of Protocols for Seed Storage. Plant Physiol. 94, 1019-1023, https://doi.org/10.1104/pp.94.3.1019

Vertucci, C.W., Roos, E.E., 1993. Theoretical Basis of Protocols for Seed Storage II. The influence of temperature on optimal moisture levels. Seed Sci. Res. 3, 201-213, https://doi.org/10.1017/S0960258500001793

Vertucci, C.W., Roos, E.E., Crane, J., 1994. Theoretical basis of protocols for seed storage III. Optimum moisture contents for pea seeds stored at different temperatures. Ann. Bot. 74, 531-540, https://doi.org/10.1006/anbo.1994.1151

Walters, C., 1998. Understanding the mechanisms and kinetics of seed aging, Seed Sci. Res. 8, 223-244, https://doi.org/10.1017/S096025850000413

Walters, C., Ballesteros, D., Vertucci, V.A., 2010. Structural mechanics of seed deterioration: Standing the test of time. Plant Sci. 179, 565-573, https://doi.org/10.1016/j.plantsci.2010.06.016

Walters, C., Maschinski, J., 2019. Conventional seed banking to support species survival in the wild: Introduction. In: CPC Best Plant Conservation Practices to Support Species Survival in the Wild, Center for Plant Conservation, Escondido, CA, USA.

Walters, C., Wheeler, L.M., Grotenhuis, J.M., 2005. Longevity of seeds stored in genebank: species characteristics, Seed Sci. Res. 15, 1-20, https://doi.org/10.1079/SSR2004195

Yang, B., Yin, Y., Liu, C., Zhao, Z., Guo, M., 2021. Effect of germination time on the compositional, functional and antioxidant properties of whole wheat malt and its end-use evaluation in cookie-making. Food Chem. 349, 129125, https://doi.org/10.1016/j.foodchem.2021.129125

Yulianti, P.K., Yuniarti, N., Aminah, A., Suita, E., Sudrajat, D., Syamsuwida, D., 2020. Seed handling of specific forest tree species: Recalcitrant and intermediate seed. In: Proc. IOP Conf. Series: Earth and Environmental Science, Changchun, China.